RESEARCH ARTICLE

Radixin Knockdown by RNA Interference Suppresses Human Glioblastoma Cell Growth *in Vitro* and *in Vivo*

Jun-Jie Qin[1], Jun-Mei Wang[1], Jiang Du[1], Chun Zeng[2], Wu Han[2], Zhi-Dong Li[2], Jian Xie[2]*, Gui-Lin Li[1]*

Abstract

Radixin, a member of the ERM (ezrin–radixin–moesin) family, plays important roles in cell motility, invasion and tumor progression. It is expressed in a variety of normal and neoplastic cells, including many types of epithelial and lymphoid examples. However, its function in glioblastomas remains elusive. Thus, in this study, radixin gene expression was first examined in the glioblastoma cells, then suppressed with a lentivirus-mediated short-hairpin RNA (shRNA) method.We found that there were high levels of radixin expression in glioblastoma U251cells. Radixin shRNA caused down-regulation of radixin gene expression and when radixin-silenced cells were implanted into nude mice, tumor growth was significantly inhibited as compared to blank control cells or non-sense shRNA cells. In addition, microvessel density in the tumors was significantly reduced. Thrombospondin-1 (TSP-1) and E-cadherin were up-regulated in radixin- suppressed glioblastoma U251 cells. In contrast, MMP9 was down-regulated. Taken together, our findings suggest that radixin is involved in GBM cell migration and invasion, and implicate TSP-1, E-cadherin and MMP9 as metastasis-inducing factors.

Keywords: Malignant glioblastoma multiform - small interference RNA - radixin - thrombospondin-1

Asian Pac J Cancer Prev, **15 (22)**, 9805-9812

Introduction

Glioblastoma (GBM) is a WHO grade IV tumor arising from the astrocytes and represents the most common type of primary central nervous system (CNS) malignancies providing for well over one half of all gliomas (Hoffman et al., 2006; Schneider et al., 2010). Current treatment methods include surgical resection, radio-surgical, external irradiation, chemotherapy (Cheng et al., 2005; Stupp et al., 2006; Wen et al., 2006), and biological therapy (Kjaergaard et al., 2005). Despite recent advances in diagnostics and treatments, prognosis for patients with this disease remains poor (Ng et al., 2007). One of the important reasons is that active cell migration and invasion of GBM cells ultimately lead to ubiquitous tumor recurrence and patient death (Xia et al., 2009). Although our understanding of GBM carcinogenesis has steadily improved, the factors that mediate GBM invasion are still poorly understood. Various studies investigate the genes and gene products involved in GBM cell migration and invasion, like matrix metalloproteinase genes, growth factors, cytokines, integrins, and cadherins (Nakada et al., 2007).

Radixin, encoded by chromosome 11 (11 exons), is a member of the ERM (ezrin-radixin-moesin) family. It functions as a membrane-cytoskeletal crosslinker in actin-rich cell surface structures and is thereby thought to be essential for cortical cytoskeleton organization, cell motility, adhesion, and proliferation (Hoeflich and Ikura, 2004). ERM proteins display a similar structural organization. They share extensive homology in their amino-terminal domain, which is called the four-point one, ezrin, radixin, moesin (FERM) domain (Gautreau et al., 2002). Spanning these globular domains is the α-helix-rich domain, termed the α-domain. Recent biophysical studies indicate that the radixin α-domain is an extremely long linear monomer with an enhanced number of electrostatic salt bridge interactions predicted to contribute synergistically to its thermal stability (Hoeflich et al., 2003). Activated radixin has been shown to join actin filaments to CD43, CD44, and ICAM1-3 cell adhesion molecules and various membrane channels and receptors, such as the Na+/H+ exchanger-3 (NHE3), cystic fibrosis transmembrane conductance regulator (CFTR), and the β2-adrenergic receptor(Tsukita and Yonemura, 1999; Bretscher et al., 2002).

Radixin is expressed in a variety of normal and neoplastic cells, including many epithelial and lymphoid cell types (Ramoni et al., 2002; Suda et al., 2011). In pancreatic carcinomas, high radixin expression levels

*[1]Department of Neuropathology, Beijing Neurosurgical Institute, [2]Department of Neurosurgery, Beijing Tiantan Hospital, Capital Medical University; China National Clinical Research Center for Neurological Diseases; Center of Brain Tumor, Beijing Institute for Brain Disorders, Beijing Key Laboratory of Brain Tumors, Beijing, China *For correspondence: liguilin2014@126.com, xiejianw@sina.com*

are associated with high metastatic, cell proliferation, survival, adhesion, and invasive potential (Chen et al., 2012). Ezrin was expressed in astrocytes in the central nervous system (CNS). Increased ezrin expression is associated with enhanced cell growth and poor malignant tumor prognosis, including gliomas (Geiger et al., 2000; Khanna et al., 2004; Tynninen et al., 2004). The observed effects of ezrin overexpression and silencing on the cell malignant transformation indicate a role for ezrin in regulating tumor metastasis and progression (Curto and McClatchey, 2004). However, the mechanisms of radixin-mediated tumor development still require further elucidation. In this study, we investigated radixin's effect on the growth and invasion ability of the glioblastoma cell line U251.

Experimental procedures

Cells and antibodies

The glioblastoma cell line U251 and normal astrocyte glial cells were purchased from the Saier Biotechnology (Tianjin, China), cultured in DMEM (GIBCO, Grand Island, NY) supplemented with 10% fetal calf serum (FCS) and 1% L-glutamine (Invitrogen, Karlsruhe, Germany), and maintained at 37°C in 5% CO_2. Rabbit polyclonal anti-radixin antibody was purchased from Upstate technology (CST, U.S.A). Mouse monoclonal anti-E-Cadherin, anti-TSP-1 antibodies, and anti-MMP9 antibodies were purchased from Cell Signaling Technology (Beverly, MA). The mouse monoclonal antibody to GAPDH was purchased from Santa Cruz Biotechnology (Santa Cruz, CA). The secondary antibodies were purchased from Saier Biotechnology (Tianjin, China).

RNA interference

A radixin (GeneBank, No. L02320) shRNA sequence was inserted into the pSIL-GFP lentivirus RNAi expression system. The shRNA-containing vectors were transfected together into 293T cells with pHelper1.0 and the lentiviral helper plasmid pHelper 2.0 to generate the respective lentiviruses. Viral stocks were collected from the transduced 293T cells and were used to infect U251 cells. The radixin nonsense shRNA sequence was ACTACCGTTGTTATAGGTG, and the radixin shRNA sequence was GACGACAAGTTAACACCTAAA. The mRNA and protein levels were measured 72 h after cells were infected.

Quantitative RT-PCR

Total cellular RNA was extracted with M-MLV-RTase (Promega, Madison, WI) according to the manufacturer's protocols. The resulting cDNA was used for PCR using the SYBR-Green Master PCR Mix (Applied Biosystem, Carlsbad, CA) in triplicates. Primers for qRT-PCR were as follows: radixin forward primer: CGAGGA AGAACGTGTAACCGAA; radixin reverse primer: TCTTGGTTTCATCTCTGGCTTG; E-Cadherin (GeneBank, No. Z13009) forward primer: CGGGAATGCAGTTGAGGATC; E-Cadherin reverse primer: AGGATGGTGTAAGCGATGGC; TSP-1 (GeneBank, No. X04665) forward primer: TGGAACTATGGGCTTGAGAAAAC; TSP-1 reverse primer: CACTGATGCAAGCACAGAAAAGA; MMP-9 (GeneBank, NM_004994.2) forward primer: TCAGGGAGACGCCCATTTC; and MMP-9 reverse primer: TGGCAGGGTTTCCCATCAG. PCR and data collection were performed on the PCR System (Takara, Shiga, Japan). All quantitation was normalized to an endogenous GAPDH control. GAPDH forward primer: AACGGATTTGGTCGTATTG; GAPDH reverse primer: GGAAGATGGTGATGGGATT. The relative quantitation value for each target gene compared to the calibrator for that target is expressed as $2^{-\Delta\Delta Ct}$, $\Delta\Delta Ct = (Ct1-Ct2)-(Ct3-Ct4)$ (Ct is the mean threshold cycle differences after normalizing to GAPDH).

Western blotting

Western blotting was performed as previously described (Guo et al., 2009). For blotting, cell lysates (30 μg protein) were separated by SDS-polyacrylamide gel electrophoresis (PAGE) using NuPAGE 4%-12% Bis-Tris gels, SDS running buffer, and NuPAGE antioxidant (Invitrogen). Proteins were transferred to polyvinylidene fluoride membrane (Invitrogen) using NuPAGE transfer buffer supplemented with NuPAGE antioxidant in 30% methanol. Standard proteins used were Magic-Mark™ XP Western protein standard (Invitrogen) for molecular weight estimations. The membrane was blocked for 1 h in room temperature in blocking solution (5% bovine serum albumin in TBS containing 0.05% Tween) and subsequently incubated with primary antibodies, Rabbit polyclonal anti-radixin (CST, U.S.A), and antibodies against E-Cadherin, TSP-1, MMP9, and GAPDH in blocking solution overnight at 4 °C. The membrane was rinsed thoroughly in TBS containing 0.05% Tween and incubated for 1 h in room temperature with horseradish peroxidase conjugated secondary antibodies in blocking solution. After subsequent rinsing, immunoreactive bands were detected using Super Signal West PICO Chemilumi Substrate (Thermo Fisher Scientific, Waltham, MA, USA) and an LAS3000 CCD camera (Fujifilm, Tokyo, Japan).

Immunocytochemical analysis

Cell pieces were dyed according to the manufacturer's protocols. The pieces were fixed in 4% paraformaldehyde 30 min in a 4°C refrigerator. Antibodies were then added, colored after being re-dyed by hematoxylin, and dehydrated by descending alcohol concentrations. The pieces were observed and documented with an Axio Imager A1 (Zeiss, Oberkochen, Germany).

Immunohistochemical analysis

Immunohistochemical assay was performed as previously described (Persson et al., 2010). The sections were de-waxed in xylene, dehydrated through graded alcohol concentration, and washed in tris buffer (pH 7.2). For antigen retrieval, the sections were immersed in citrate buffer (pH 6.2) at 90°C for 1h using a water bath and then incubated with 3% hydrogen peroxide in methanol for 15 min to block endogenous peroxidase activity. After washing twice in tris buffer, sections were incubated 3-4 h at room temperature separately with

polyclonal antibody. Following washing in tris buffer, the sections were sequentially incubated with biotinylated link secondary antibody for 30 min in each. The sections were washed twice again in tris buffer and incubated with the chromogen diaminobenzidine-tetrahydrochloride substrate, followed by counterstaining in hematoxylin. The sections were mounted in DPX mountant. Parallel control slides were run with all batches, including positive and negative controls.

MTT assay

MTT assay was performed as previously described (Chen et al., 2010). Viable cells (2×10^5 cells/ml) were plated into 96-well plates (100 μl complete medium/well) and cultured at 37°C in 5% CO_2. At different time points, MTT reagent (5 mg/ml) (DingGuo Biotech, Beijing, China) was added (20 μl per well) and incubated at 37°C for 4h. The reaction was stopped with 100 μl DMSO and the optical density was determined at OD570 nm on a multi-well plate reader.

Cell Cycle Assay

Cell cycle analysis was performed by flow cytometry as described previously (Meng et al., 2010). 5×10^5 cells were plated in 60 mm dishes and cultured for 2 days. Cells were collected by trypsinization, fixed with 95% ethanol, washed with PBS, resuspended in 1 mL of 0.01M PBS with RNase and 50 μg/mL propidium iodide, incubated for 20 min in the dark at room temperature, and analyzed by flow cytometry using a FACS Calibur (Becton Dickinson, Bedford, MA).

Apoptotic cell detection

Cells were stained with fluorescein isothiocyanate (FITC) labeled annexin-V and propidium iodide (PI) stain simultaneously to discriminate intact cells (annexin-/PI-) from apoptotic cells (annexin+/PI-) and necrotic cells (annexin+/PI+). A total of 2.0×10^5 cells were washed twice with ice-cold PBS and incubated for 30 min in a binding buffer (1 μg/ml PI and 1 μg/ml FITC labeled annexin-V), respectively. FACS analysis for annexin-V and PI staining was performed by flow cytometer.

Adhesion assay

96-well plates were coated 1 h at 37 °C with 20 μg/ml of fibronectin (FN) and blocked with 0.5% BSA for 1 h at room temperature. Then, 4×10^5 /ml cells were seeded in each well and incubated at 37°C for 30 min in 5% CO_2. After incubation, unbound cells were removed along with the culture medium. Remaining adherent cells were colored for 15 min with 0.5% violet crystal and fixed with 20% methanol. After washing with PBS, adherent cells were lysed with 1% SDS. Adhesion was quantified with spectrophotometric optic density measurement at 550 nm.

Invasion assay

Invasion assay was performed as previously described (Albini et al., 1987). In short, cells were harvested and washed with serum-free medium. 1×10^5 cell suspension was then added into the matrigel transwells, with 200 μl of culture medium containing 10ng/ml ECM as the chemoattractant in the lower chamber. Cells that invaded through the matrigel membrane were stained and counted after 24h incubation at 37°C.

Tumor growth in nude mice

Female BALB/c nude mice (obtained from Beijing HuaFuKang Biotechnology Co., LTD, Beijing; body weight, 15 to 17g) were bred under specified pathogen-free conditions (26°C, 70% relative humidity, and a 12h light/12h dark cycle) in a germ-free environment with free access to food and water. The logarithmically growing cells were trypsinized and resuspended in D-Hanks solution. 2×10^6 cells in 0.1 ml were injected subcutaneously into the mice's left flanks. Experimental and control groups had at least 10 mice each. Tumors were measured twice weekly with microcalipers, and the tumor volume was calculated according to the formula: V (volume)=LW2×π/6, where "L" represents the greatest length and "W" represents the perpendicular width (Butler et al., 1986). The animals were sacrificed by cervical dislocation under light ether anesthesia after 4 weeks. The tumors were excised and weighed. Part tumor specimens were fixed in 4% formaldehyde, embedded in paraffin, and cut in 4 μm sections for immunohistochemical analysis (IHC). Parts were kept at -80 °C refrigeration and used for Quantitative RT-PCR (qRT-PCR) and Western blot detection (WB). All procedures met national guidelines for care and use of laboratory animals and were approved by the Institutional Animal Care and Use Committee of Capital Medical University, Beijing, China.

Quantification of tumor microvessel density and in situ TUNEL assay for apoptotic cells

Tumor microvessel densities (MVD) were quantified by anti-CD31 immunohistochemistry as previously described (Singh et al., 2010). Apoptotic cells in tumor samples were identified by terminal deoxyribonucleotidyl transferase dUTP nick end fluorescein labeling (TUNEL) assay according to the manufacturer's instructions (In situ Cell Death Detection Kit, Roche, Indianapolis, IN). The number of apoptotic cells was evaluated by counting the positive (brown-stained) cells in 10 random fields (×200).

Statistical analysis

Each experiment was performed three to four times. All data were expressed as mean±SD. Statistical analysis was performed with SPSS 13.0 software (SPSS Inc., Chicago, IL). Comparisons between groups were conducted using one-way analysis of variance (ANOVA) or Student's t test. P values<0.05 were considered statistically significant.

Results

Radixin mRNA and protein expression in glioblastoma U251 cells

To investigate radixin expression, we compared the glioblastoma U251 with normal glial cells by IHC, WB, and qRT-PCR, as shown in Figure 1. There are radixin expressions in normal glial cells at both the mRNA and protein levels and higher radixin expression levels in glioblastoma cells compared to normal glial cells.

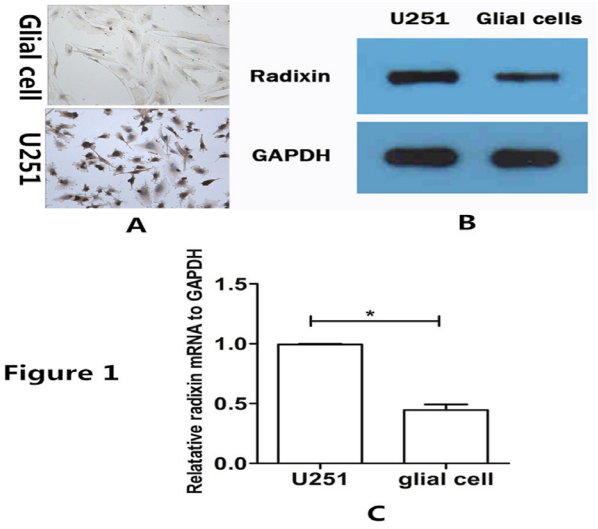

Figure 1

Figure 1. Radixin mRNA and Protein Expressions in Glioblastoma U251 Cells. Higher radixin expression in glioblastoma U251 cells compared with normal astrocyte glial cells. **(A)** The numbers of staining cells were increased markedly on U251 cells compared with normal astrocyte glial cells; **(B)** WB shows radixin protein level in U251 cells is higher when compared; **(C)** The radixin mRNA level is higher compared with normal astrocyte glial cells. Results represent the mean±SD of the experiments. *p<0.05

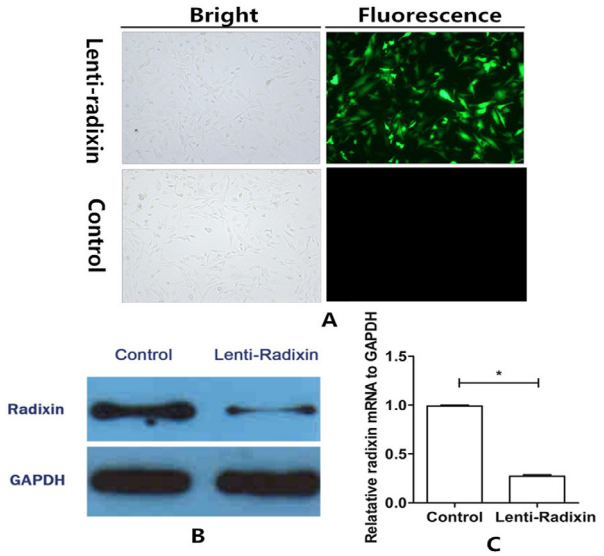

Figure 2. Efficient shRNA Delivery into Glioblastoma U251 Cells and Stable Suppressing of Radixin in U251 Cells. **(A)** High efficiency of transduction with fluorescent shRNA (green) in U251 cells was easily identified 48h post-transduction. Transduction comparison of the two groups. Mock: blank control; Lenti-radixin: radixin shRNA; **(B)** The radixin protein level was down-regulated stably by radixin shRNA in U251 cells; **(C)** The radixin mRNA level was down-regulated stably by radixin shRNA in U251 cells. Results represent the mean±SD of two independent experiments.*p<0.05

Reduction of radixin mRNA and protein expression by shRNA in vitro

To investigate radixin's biological role in U251 cells, we knocked down radixin transcript by employing shRNA technology. ShRNA to radixin was constructed into pSIL-GFP vector using a lentivirus transduction system, radixin mRNA and protein expression by shRNA *in vitro* also reduced, as shown in Figure 2.

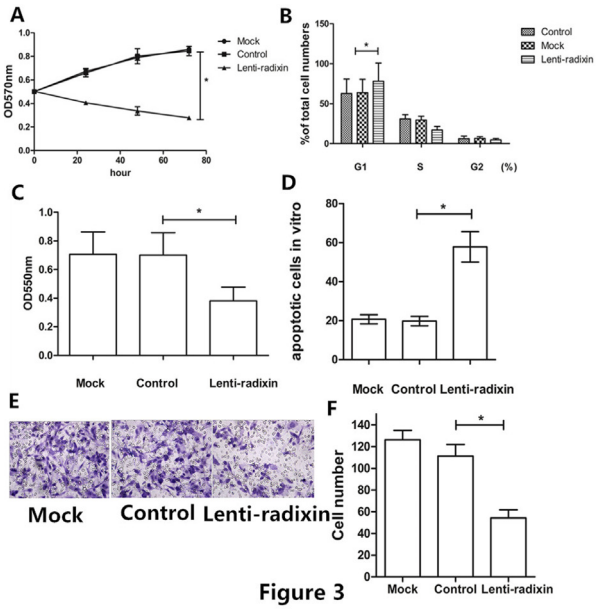

Figure 3

Figure 3. Down-Regulation of Radixin Inhibits Proliferation, Promotes Apoptosis, Inhibits the Adhesion and Invasion of U251 Cells. **(A)** U251 cell proliferation was inhibited when treated with radixin shRNA by MTT assay; **(B)** The proportion of U251 cells increased with G1 phase as a consequence of decreased radixin expression; **(C)** Down-regulation of radixin inhibits glioblastoma U251 cell adhesion. The number of adherent living cells was significantly lower in the lenti-radixin group than in the mock group and control group; **(D)** Down-regulation of radixin promotes glioblastoma U251 cell apoptosis; **(E)** Matrigel-coated transwell chambers were used to detect cell invasion and representative fields were photographed; **(F)** The decrease in the numbers of invasive cells in the Lenti-radixin group compared to those of the Mock or Control group was statistically significant. Results represent the mean±SD of three independent experiments. *p<0.05

Radixin down-regulation inhibited glioblastoma U251 cell proliferation

Using radixin cell down-regulation, we first tested U251 cell growth changes using the MTT assay. Results showed a significant cell growth decrease and indicated that cell proliferation was inhibited after transduction with radixin shRNA (Figure 3A). The flow cytometry assay showed that the proportion of cells in the G1 phase was significantly increased and those in the G2 and S phases were decreased after transduction with radixin shRNA (Figure 3B). These results indicated that radixin could enhance the U251 cell growth ability *in vitro*.

Radixin down-regulation promoted glioblastoma U251 cell apoptosis

To determine the effects of radixin's down-regulation on the radixin-induced apoptosis in U251 cells, the apoptosis rate was evaluated by flow cytometry analysis. As shown in Figure 3D, the radixin-induced apoptosis effects were investigated in cells treated with radixin shRNA as well as cells in blank controls and cells treated with nonsense shRNA. We found a significantly elevated apoptosis percentage in cells transfected with radixin shRNA compared to blank control cells (p=0.045), while there was no significant difference between blank controls and cells transfected with nonsense shRNA (p>0.05).

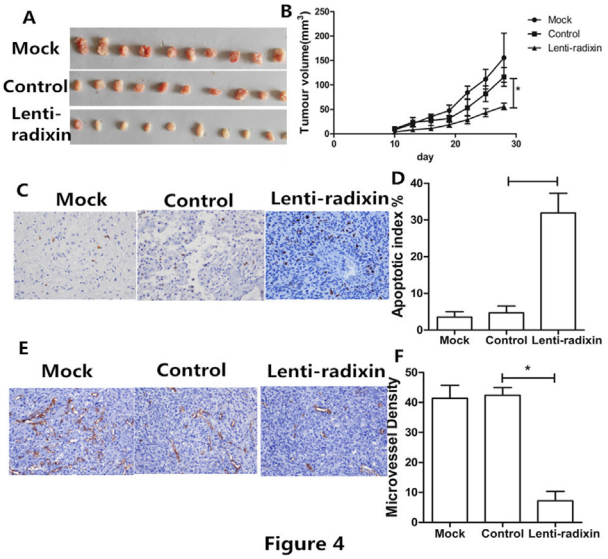

Figure 4

Figure 4. Down-Regulation of Radixin Reduces Tumor Growth, Increases Apoptosis and Decreases Microvessel Density of Glioblastoma *in Vivo*. Glioblastoma cells (Control, Mock, or Lenti-radixin) were subcutaneously injected into the left flank regions of nude mice. **(A)** Tumor volumes were measured every three days with a caliper and were calculated; using the formula π/6×(smaller diameter) 2×(larger diameter). **(B)** Tumor volumes from day 0 to day 28 (n=10). Lenti-radixin group growth was significantly reduced ($p<0.05$) compared with Control or Mock group; **(C)** Representative photographs of decreases in microvessel density from the tumor sections examined by TUNEL assay; **(D)** The data present the average number of apoptotic cells±SD; **(E)** Immunohistochemical staining for microvessels with anti-CD31. The representative pictures are shown at 200× magnification; **(F)** Microvessel density was quantitated microscopically with a 5×5 reticle grid at 400× magnification. The values are mean±SD.*$p<0.05$

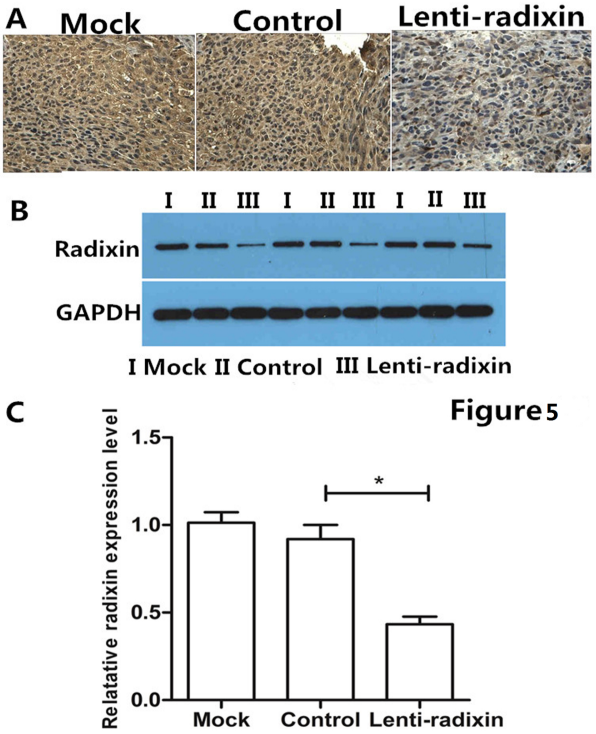

Figure 5

Figure 5. Suppressed Radixin mRNA and Protein in Lenti-radixin Group *in Vivo*. **(A)** Representative photographs of the tumor sections examined by microscopy. Immunohistochemical staining for radixin. The representative pictures are shown at 400× magnification; **(B)** The radixin protein level was down-regulated by radixin shRNA *in vivo*; **(C)** The radixin mRNA level was down-regulated by radixin shRNA *in vivo*. Results represent the mean±SD of three independent experiments. *$p<0.05$

Radixin down-regulation inhibited the adhesion and invasion of glioblastoma U251 cells

In the cell adhesion *in vitro* experiment, the number of adherent living cells was significantly lower in the radixin shRNA group (Lenti-radixin) than in the nonsense shRNA group (Control) and blank control group (Mock) (Figure 3C). These results suggest that radixin shRNA induces the loss of cell adhesion to the matrix. Since two critical steps are involved in metastasis, adhesion and invasion, we next examined whether radixin can affect U251 cell invasion activity by the matrigel invasion assay. Cell invasive activity was also dramatically decreased in the Lenti-radixin cells compared with the Mock or Control cells. The average cell number invading to the lower chamber for 24h was 54.33±7.51/HPF in the radixin shRNA cells, compared to 126.33±8.62/HPF in the Mock cells or 111.33±10.69/HPF in the Control cells. The quantitative analysis showed that the number of radixin shRNA cells invading to the lower chamber was decreased by 57.01% compared to the Mock cells ($p<0.05$), while there was no significant difference between Mock and Control cells ($p>0.05$) (Figure 3E, 3F).

Radixin down-regulation resulted in reduced tumor growth and angiogenesis

To specifically determine radixin's role in tumor development, Lenti-Radixin, Control, or Mock cells were injected into the left flank regions of nude mice (n=10/group). All of the mice developed tumors. Four weeks after tumor injection, tumor volumes were measured. Subcutaneous tumors formed from Lenti-Radixin cells were significantly smaller compared with the Mock or Control cells (Control, 155.85±50.25mm3; Mock, 116.36±19.25 mm3; Lenti-Radixin, 56.18 ± 6.40 mm3) (Figure 4A, 4B). Additionally, Lenti-Radixin tumors had significantly increased numbers of TUNEL-positive cells ($p<0.05$) (Figure 4C, 4D).

One possible mechanism for decreased tumor growth is attenuated neovascularization. To determine whether radixin down-regulation could potentially disrupt the neovascularization, we examined vascularity in tumors. Staining on Lenti-Radixin tumor sections showed a 4.7-fold decrease in the number of blood vessels compared with Mock or Control tumors (Figure 4E, 4F).

Reduction of radixin mRNA and protein expression by shRNA in vivo

Lenti-Radixin tumors had significantly decreased Radixin expression compared to Mock or Control tumors ($p<0.05$) (Figure 5). Similar results were found *in vitro*.

Thrombospondin-1 (TSP-1), MMP9, and E-Cadherin were regulated in Lenti-radixin U251 cells

To determine the mechanism(s) by which radixin regulates tumor growth and progression, we examined

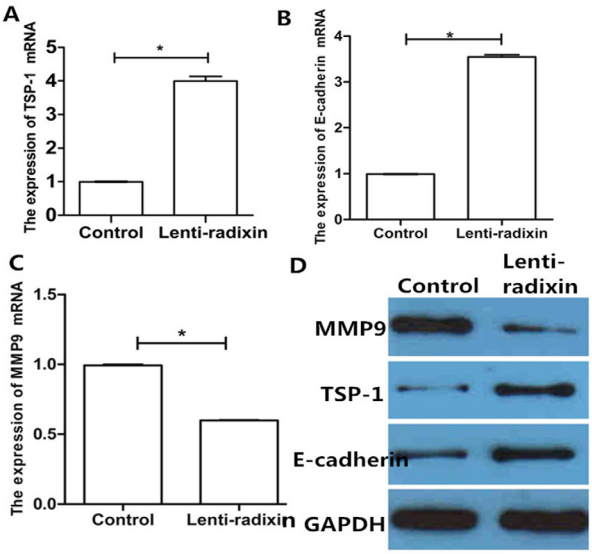

Figure 6. Thrombospondin-1 (TSP-1), E-Cadherin, and MMP9 Were Regulated in Lenti-radixin U251 Cells. (AB) The TSP-1 and E-Cadherin mRNA levels were up-regulated by radixin shRNA in U251 cells; **(C)** MMP9 mRNA levels were down-regulated by radixin shRNA in U251 cells; **(D)** The TSP-1 and E-Cadherin protein levels were up-regulated by radixin shRNA in U251 cells. MMP9 protein levels were down-regulated by radixin shRNA in U251 cells. Results represent the mean±SD of two independent experiments. *$p<0.05$

potential radixin-regulated molecules. As we know, E-cadherin plays a central role in heterotypic epithelial cell-cell adhesion and maintaining epithelial cell colony integrity (Takeichi, 1993). TSP-1 is a potent inhibitor of neovascularization that limits tumor growth (Castle et al., 1997). MMP9 is an important protease of the matrix metalloproteinase (MMPs) family in glioblastoma biology, which can degrade the extracellular matrix (ECM). MMP9 is up-regulated in glioma cell lines and human specimens (Uhm et al., 1997; Forsyth et al., 1998; Forsyth et al., 1999). MMPs are overexpressed not only by glioma cell lines but also by the tumor vasculature, suggesting a relevant role in angiogenesis induction and regulation (Liotta et al., 1991; Hanahan and Folkman, 1996). In this study, Western blot analysis and quantitative RT-PCR revealed that TSP-1 and E-Cadherin were dramatically up-regulated but MMP9 was dramatically down-regulated in cells transfected with radixin shRNA (Figure 6). Those results suggest that TSP-1 and E-Cadherin expression down-regulation and MMP9 expression up-regulation might participate in radixin-mediated tumor growth and progression.

Discussion

Radixin is a member of the ERM (ezrin-radixin-moesin) family and shares the common membrane-binding N-terminal FERM domain with band-4.1 family members (Turunen et al., 1994). By organizing membrane-cytoskeleton-associated complexes and creating specialized membrane domains, the ERM proteins regulate cellular activities like survival, adhesion, and migration/invasion, all of which are important during tumor development and progression (Bretscher et al., 2002; McClatchey, 2003; Chen et al., 2012). Mice lacking radixin are characterized by hepatocyte apical microvilli breakdown, which ultimately results in mild liver injury similar to human conjugated hyperbilirubinemia in Dubin-Johnson syndrome (Kikuchi et al., 2002). High ERM expression levels were observed in many tumor cell lines, such as the breast carcinoma and osteosarcoma cell line (Khanna et al., 2004; Revillion et al., 2008). However, its role and mechanisms remain elusive.

Our results showed that radixin was expressed in astrocytes in the central nervous system (CNS), radixin expression is higher in glioblastoma U251 cells compared with normal astrocytes cells, and knocking down radixin resulted in an inhibition of cell proliferation and survival. Additionally, we observed decreased Lenti-radixin U251 cell adhesion and invasion. We established experimental mice models and showed that radixin knock-down regulated primary tumor growth, angiogenesis, and progression. Hence, our study's results suggest an important correlation between radixin expression and glioblastoma cancer growth and invasion. So, increased radixin expression is associated with enhanced cell growth and poor malignant GBM prognosis.

Increased cell proliferation and decreased cell death play a pivotal role in tumor progression. Any decreased tumor growth of radixin-suppressed cells may be due to their decreased response to cell proliferation, adhesion, survival, or invasion. The present *in vitro* data reveals that suppressing radixin results in a significant decrease in proliferation. Another important finding of this study was the enhanced apoptosis of radixin-suppressed cells. An apoptotic property of these cells was observed both *in vitro* and in tumor tissues. Our results are consistent with previous finding in hippocampal pyramidal cells (Paglini et al., 1998). The observed effects of radixin silencing on the GBM cell transformation indicate a role for radixin in regulating tumor metastasis and progression. Our results are consistent with previous finding in Ezrin (Curto and McClatchey, 2004).

Cell invasion into the surrounding tissue is a multi-step action that requires cell-cell contact, cell motility, and extracellular matrix (ECM) degradation by matrix metalloproteinases (MMPs). Malignant tumor cells display varying degrees of resistance to detachment, generating cell-extracellular matrix interactions related to the adhesion complex. This property contributes to tumorigenesis and metastasis (Frisch and Francis, 1994; Chen et al., 2012). Our *in vitro* study showed significant differences in adhesion and invasion between radixin shRNA and control cells. Radixin is a cytoskeletal protein that might affect the cytoskeletal element assembly at the cytoplasmic face of the membrane and the nuclear skeleton, which would facilitate cell invasion. These results agree with another report where ERM stable knockdown by shRNA reduced *in vitro* human SGC-7901 cell migration and invasion (Ou-Yang et al., 2011). Angiogenesis is another essential step for tumor growth and metastasis. Our immunohistochemistry results support that primary tumor vasculature contributed to *in vivo* differences between Lenti-radixin and nonsense shRNA control tumors.

E-cadherin was first discovered in 1995 by Berx (Berx et al., 1995). It is a calcium-dependent cell-cell adhesion molecule with pivotal roles in epithelial cell behavior, tissue development, and cancer growth suppression (Stemmler, 2008; van Roy and Berx, 2008; Sun et al., 2013). TSP-1 is a potent neovascularization inhibitor that limits tumor growth (Castle et al., 1997) and stimulates apoptosis and growth inhibition in neovascular endothelial cell (Jimenez et al., 2000; Lawler et al., 2001). TSP-1 is also reported to inhibit invasion (Moon et al., 2005). Our results showed that E-cadherin and TSP-1 expression levels were markedly increased in the Lenti-radixin cells. Therefore, radixin high expression can down-regulation TSP-1 and E-Cadherin expression, and down-regulation of E-Cadherin lost the ability of cell-cell adhesion, improved the cell mobility, may induced glioblastoma cell growth and invasion. Down-regulation of TSP-1 also weakened the ability of inhibition tumor invasion.

Matrix metalloproteinase (MMPs) constitute some of the most important proteases in glioblastoma biology. In fact, the ability of glioblastoma to infiltrate the surrounding brain parenchyma and induce neo-angiogenesis strictly depends on proteases. Such proteases are capable of degrading the extracellular matrix (ECM) and the basal membranes, thus opening migratory pathways for endothelial and tumor cells. Additionally, proteases can alter cell adhesion properties interfering with cell surface receptor activities, like integrins or cadherins, which usually modulate cell motility. Degrading the ECM, proteases can release growth factors and other molecule involved in tumor angiogenesis, growth, and invasion. Various types of MMPs, such as MMP9, have been shown to be up-regulated in glioma cell lines and human specimens (Uhm et al., 1997; Forsyth et al., 1998; Forsyth et al., 1999). MMPs are overexpressed not only by glioma cell lines but also by the tumor vasculature, suggesting a relevant role in angiogenesis induction and regulation (Liotta et al., 1991; Hanahan and Folkman, 1996). MMP9 are overexpressed also in many other tumors, such as in osteosarcomas (Jin et al., 2013), breast cancer (Darakhshan et al., 2013), cholangiocarcinoma (Kidoikhammouan et al., 2013), human fibrosarcoma cell (Yahayo et al., 2013), which all are overexpressed, suggesting a relevant role in tumor angiogenesis, growth, and invasion. Our results showed that MMP9 expressions were markedly decreased in Lenti-radixin cells *in vitro*. Therefore, high expression of radixin induced up-regulation of MMP9 expression, enhanced the capable of MMP9 in degrading the extracellular matrix (ECM) and the basal membranes, alter cell adhesion properties to cell-cell adhesion, promoted and accelerated the growth and invasion of glioblastoma cells.

Glioblastoma multiform (GBM or grade IV astrocytoma), or simply glioblastoma, represents the most aggressive and malignant entity. These clinic-pathological features reflect the biology of GBMs, which is characterized by high proliferation rate, low apoptosis, marked invasiveness, and hyper-vascularization. Single biological agents have failed to change significantly the prognosis of glioblastoma patients. The explanation for these still poor results probably lies in the highly aberrant glioblastoma environment. The molecular and genetic alterations, which are a sustaining scenario, have only been partly clarified, also because the definition of 'multiform' reflects the macroscopic appearance of the neoplasm as well as its molecular heterogeneity. Our results reflected almost all of the biology of GBMs, and showed the important role of radixin in GBM, introduced knockdown of radixin can suppress the proliferation and invasion of GBM. So knockdown of radixin may be one of the important and useful methods to treat GBM.

In conclusion, we detected high expression of radixin in the glioblastoma cells first, and successfully suppressed the radixin protein and mRNA expression in glioblastoma U251 cells. We found that changes in the radixin protein and mRNA levels were correlated with changes in the proliferation, apoptosis, adhesion, and invasion. Based on these results, we propose that radixin might play a critical role in glioblastoma progression. Down-regulating TSP-1 and E-Cadherin expressions and up-regulating MMP9 expression may be involved in this role. These results indicate that blocking radixin function may represent a novel and effective strategy for preventing glioblastoma progression.

The study's limitations include the possibility of off-target shRNA effects, differential radixin expression between normal glial cells versus GBM cells should be analyzed in multiple lines. Ideally, this should be done in primary patient samples too. These issues should be addressed in the future.

Acknowledgements

This work was supported by grants from the "Capital Health Project" (Z131100006813011), the "basic-clinical scientific research cooperation foundation of the capital medical university" (13JL04), "National Key Technology Research and Development Program of the Ministry of Science and Technology of China" (2013BAI09B03), and "Beijing Institute for Brain Disorders" (BIBD-PXM2013_014226_07_000084).

References

Albini A, Iwamoto Y, Kleinman HK, et al (1987). A rapid *in vitro* assay for quantitating the invasive potential of tumor cells. *Cancer Res*, **47**, 3239-45.

Berx G, Staes K, van Henqel J, et al (1995). Cloning and characterization of the human invasion suppressor gene E-cadherin (CDH1). *Genomics*, **26**, 281-9.

Bretscher A, Edwards K, Fehon RG (2002). ERM proteins and merlin: integrators at the cell cortex. *Nat Rev Mol Cell Biol*, **3**, 586-99.

Butler WB, Berlinski PJ, Hillman RM, et al (1986). Relation of *in vitro* properties to tumorigenicity for a series of sublines of the human breast cancer cell line MCF-7. *Cancer Res*, **46**, 6339-48.

Castle VP, Dixit VM, Polverini PJ (1997). Thrombospondin-1 suppresses tumorigenesis and angiogenesis in serum- and anchorage-independent NIH 3T3 cells. *Lab Invest*, **77**, 51-61.

Chen J, Xie F, Zhang L, et al (2010). iASPP is over-expressed in human non-small cell lung cancer and regulates the proliferation of lung cancer cells through a p53 associated pathway. *BMC Cancer*, **10**, 694.

Chen SD, Song MM, Zhong ZQ, et al (2012). Knockdown of radixin by RNA interference suppresses the growth of human pancreatic cancer cells *in vitro* and *in vivo*. *Asian Pac J Cancer Prev*, **13**, 753-9.

Cheng CL, Johnson SP, Keir ST, et al (2005). Poly (ADP-ribose) polymerase-1 inhibition reverses temozolomide resistance in a DNA mismatch repair-deficient malignant glioma xenograft. *Mol Cancer Ther*, **4**, 1364-8.

Curto M, McClatchey AI (2004). Ezrin a metastatic detERMinant? *Cancer Cel*, **5**,113-4.

Darakhshan S, Bidmeshkipour A, Khazaei M, et al (2013). Synergistic effects of tamoxifen and tranilast on VEGF and MMP-9 Regulation in cultured human breast cancer cells. *Asian Pac J Cancer Prev*, **14**, 6869-74.

Forsyth PA, Laing TD, Gibson AW, et al (1998). High levels of gelatinase-B and active gelatinase-A in metastatic glioblastoma. *J Neurooncol*, **36**, 21-9.

Forsyth PA, Wong H, Laing TD, et al (1999). Gelatinase-A (MMP-2), gelatinase-B (MMP-9) and membrane type matrix metalloproteinase-1 (MT1-MMP) are involved in different aspects of the pathophysiology of malignant gliomas. *Br J Cancer*, **79**, 1828-35.

Frisch SM, Francis H (1994). Disruption of epithelial cell-matrix interactions induces apoptosis. *J Cell Biol*, **124**, 619-26.

Gautreau A, Louvard D, Arpin M (2002). ERM proteins and NF2 tumor suppressor: the Yin and Yang of cortical actin organization and cell growth signaling. *Curr Opin Cell Biol*, **14**, 104-9.

Geiger KD, Stoldt P, Schlote W, et al (2000). Ezrin immunoreactivity is associated with increasing malignancy of astrocytic tumors but is absent in oligodendrogliomas. *Am J Pathol*, **157**, 1785-93.

Guo H, Ma Y, Zhang B, et al (2009). Pivotal advance: PKCzeta is required for migration of macrophages. *J Leukoc Biol*, **85**, 911-8.

Hanahan D, Folkman J (1996). Patterns and emerging mechanisms of the angiogenic switch during tumorigenesis. *Cell*, **86**, 353-64.

Hoeflich KP, Ikura M (2004). Radixin: cytoskeletal adopter and signaling protein. *Int J Biochem Cell Biol*, **36**, 2131-6.

Hoeflich KP, Tsukita S, Hicks L, et al (2003). Insights into a single rod-like helix in activated radixin required for membrane-cytoskeletal cross-linking. *Biochemistry*, **42**, 11634-41.

Hoffman S, Propp JM, McCarthy BJ (2006). Temporal trends in incidence of primary brain tumors in the United States, 1985-1999. *Neuro Oncol*, **8**, 27-37.

Jimenez B, Volpert OV, Crawford SE, et al (2000). Signals leading to apoptosis-dependent inhibition of neovascularization by thrombospondin-1. *Nat Med*, **6**, 41-8.

Jin J, Cai L, Liu ZM, et al (2013). miRNA-218 Inhibits Osteosarcoma Cell Migration and Invasion by Down-regulating of TIAM1, MMP2 and MMP9. *Asian Pac J Cancer Prev*, **14**, 3681-4.

Khanna C, Wan X, Bose S, et al (2004). The membrane-cytoskeleton linker ezrin is necessary for osteosarcoma metastasis. *Nat Med*, **10**, 182-6.

Kidoikhammouan S, Seubwai W, Tantapotinan N, et al (2013). TNP-470, A methionine aminopeptidase-2 inhibitor, inhibits cell proliferation, migration and invasion of human cholangiocarcinoma Cells *In Vitro*. *Asian Pac J Cancer Prev*, **13**, 155-60.

Kikuchi S, Hata M, Fukumoto K, et al (2002). Radixin deficiency causes conjugated hyperbilirubinemia with loss of Mrp2 from bile canalicular membranes. *Nat Gene*, **31**, 320-5.

Kjaergaard J, Wang LX, Kuriyama H, et al (2005). Active immunotherapy for advanced intracranial murine tumors by using dendritic cell-tumor cell fusion vaccines. *J Neurosurg* **103**, 156-64.

Lawler J, Miao WM, Duquette M, et al (2001). Thrombospondin-1 gene expression affects survival and tumor spectrum of p53-deficient mice. *Am J Pathol*, **159**, 1949-56.

Liotta LA, Steeg PS, Stetler-Stevenson WG (1991). Cancer metastasis and angiogenesis: an imbalance of positive and negative regulation. *Cell*, **64**, 327-36.

McClatchey AI (2003). Merlin and ERM proteins: unappreciated roles in cancer development? *Nat Rev Cancer*, **3**, 877-83.

Meng Y, Lu Z, Yu S, et al (2010). Ezrin promotes invasion and metastasis of pancreatic cancer cells. *J Transl Med*, **8**, 61.

Moon Y, Bottone FGJr, McEntee MF, et al (2005). Suppression of tumor cell invasion by cyclooxygenase inhibitors is mediated by thrombospondin-1 via the early growth response gene Egr-1. *Mol Cancer Ther,* **4**, 1551-8.

Nakada M, Nakada S, Demuth T, et al (2007). Molecular targets of glioma invasion. *Cell Mol Life Sci*, **64**, 458-78.

Ng SS, Cheung YT, An XM, et al (2007). Cell cycle-related kinase: a novel candidate oncogene in human glioblastoma. *J Natl Cancer Inst,* **99**, 936-48.

Ou-Yang M, Liu H R, Zhang Y, et al (2011). ERM stable knockdown by siRNA reduced *in vitro* migration and invasion of human SGC-7901 cells. *Biochimie*, **93**, 954-61.

Paglini G, Kunda P, Quiroga S, et al. (1998). Suppression of radixin and moesin alters growth cone morphology, motility, and process formation in primary cultured neurons. *J Cell Biol*, **143**, 443-55.

Persson A, Lindwall C, Curtis MA, et al (2010). Expression of ezrin radixin moesin proteins in the adult subventricular zone and the rostral migratory stream. *Neuroscience*, **167**, 312-22.

Ramoni C, Luciani F, Spadaro F, et al (2002). Differential expression and distribution of ezrin, radixin and moesin in human natural killer cells. *Eur J Immunol*, **32**, 3059-65.

Revillion F, Lhotellier V, Hornez L, et al (2008). Real-time reverse-transcription PCR to quantify a panel of 19 genes in breast cancer: relationships with sentinel lymph node invasion. *Int J Biol Markers*, **23**, 10-7.

Schneider T, Mawrin C, Scherlach C, et al (2010). Gliomas in adults. *Dtsch Arztebl Int*, **107**, 799-807.

Singh S, Sadanandam A, Varney ML, et al (2010). Small interfering RNA-mediated CXCR1 or CXCR2 knock-down inhibits melanoma tumor growth and invasion. *Int J Cancer*, **126**, 328-36.

Stemmler MP (2008). Cadherins in development and cancer. *Mol Biosyst*, **4**, 835-50.

Stupp R, Hegi M E, van den Bent MJ, et al. (2006). Changing paradigms-an update on the multidisciplinary management of malignant glioma. *Oncologist*, **11**, 165-80.

Suda J, Zhu L, Karvar S (2011). Phosphorylation of radixin regulates cell polarity and Mrp-2 distribution in hepatocytes. *Am J Physiol Cell Physiol*, **300**, 416-24.

Sun XJ, Liu H, Zhang P, et al (2013). miR-10b promotes migration and invasion in nasopharyngeal carcinoma cells. *Asian Pac J Cancer Prev*, **14**, 5533-7.

Takeichi M (1993). Cadherins in cancer: implications for invasion and metastasis. *Curr Opin Cell Biol*, **5**, 806-11.

Tsukita S, Yonemura S (1999). Cortical actin organization: lessons from ERM (ezrin/radixin/moesin) proteins. *J Biol Chem*, **274**, 34507-10.

Turunen O, Wahlstrom T, Vaheri A (1994). Ezrin has a COOH-terminal actin-binding site that is conserved in the ezrin protein family. *J Cell Biol*, **126**, 1445-53.

Tynninen O, Carpen O, Jaaskelainen J, et al (2004). Ezrin expression in tissue microarray of primary and recurrent gliomas. *Neuropathol Appl Neurobiol*, **30**, 472-7.

Uhm JH, Dooley NP, Villemure JG, et al (1997). Mechanisms of glioma invasion: role of matrix-metalloproteinases. *Can J Neurol Sci*, **24**, 3-15.

van Roy F and Berx G (2008). The cell-cell adhesion molecule E-cadherin. *Cell Mol Life Sci*, **65**, 3756-88.

Wen PY, Yung WK, Lamborn KR, et al (2006). Phase I/II study of imatinib mesylate for recurrent malignant gliomas: North American Brain Tumor Consortium Study 99-08. *Clin Cancer Res*, **12**, 4899-907.

Xia H, Qi Y, Ng SS, et al (2009). microRNA-146b inhibits glioma cell migration and invasion by targeting MMPs. *Brain Res*, **1269**, 158-65.

Yahayo W, Supabpho A, Supabphol R (2013). Suppression of human fibrosarcoma cell metastasis by Phyllanthus emblica extract *in Vitro*. *Asian Pac J Cancer Prev*, **14**, 6863-7.